AEDC-TR-69-184

AXIALLY SYMMETRIC, INVISCID, REAL GAS, NON-ISOENERGETIC FLOW SOLUTION BY THE METHOD OF CHARACTERISTICS

John H. Fox

ARO, Inc.

January 1970

ARNOLD ENGINEERING DEVELOPMENT CENTER
AIR FORCE SYSTEMS COMMAND
ARNOLD AIR FORCE STATION, TENNESSEE

NOTICES

When U. S. Government drawings specifications, or other data are used for any purpose other than a definitely related Government procurement operation, the Government thereby incurs no responsibility nor any obligation whatsoever, and the fact that the Government may have formulated, furnished, or in any way supplied the said drawings, specifications, or other data, is not to be regarded by implication or otherwise, or in any manner licensing the holder or any other person or corporation, or conveying any rights or permission to manufacture, use, or sell any patented invention that may in any way be related thereto.

Qualified users may obtain copies of this report from the Defense Documentation Center.

References to named commercial products in this report are not to be considered in any sense as an endorsement of the product by the United States Air Force or the Government.

ERRATA

AEDC-TR-69-184, January 1970

AXIALLY SYMMETRIC, INVISCID, REAL GAS,
NON-ISOENERGETIC FLOW SOLUTION BY
THE METHOD OF CHARACTERISTICS

John H. Fox, ARO, Inc.

Arnold Engineering Development Center
Air Force Systems Command
Arnold Air Force Station, Tennessee

The denominator of Eq. (55), p. 24, of the referenced report should be

$$\bar{u}_1^2 - \bar{a}_1^2$$

The denominator of Eq. (56), p. 24, should be

$$\bar{u}_2^2 - \bar{a}_2^2$$

The last line on p. 26 should be

$$X_4 = (1/\bar{\rho}_3\bar{u}_3)\bar{Q}_3(Z_4 - Z_3) + h_3 + \bar{v}_3 v_3 + \bar{u}_3 u_3$$

The denominator of Eq. (62), p. 31, should be

$$\bar{u}_1^2 - \bar{a}_1^2$$

Equation (64), p. 31, should be

$$\bar{\rho}_3\bar{v}_3 v_4 + \bar{\rho}_3\bar{u}_3 u_4 = \bar{\rho}_3\bar{v}_3 v_3 + \bar{\rho}_3\bar{u}_3 u_3$$

The denominator of the last equation, p. 36, should be

$$\bar{u}^2 - \bar{a}^2$$

AXIALLY SYMMETRIC, INVISCID, REAL GAS, NON-ISOENERGETIC FLOW SOLUTION BY THE METHOD OF CHARACTERISTICS

John H. Fox
ARO, Inc.

FOREWORD

The work reported herein was done at the request of Headquarters, Arnold Engineering Development Center (AEDC), under Program Element 65401F.

The results of the research were obtained by ARO, Inc. (a subsidiary of Sverdrup & Parcel and Associates, Inc.), contract operator of AEDC, Air Force Systems Command (AFSC), Arnold Air Force Station, Tennessee, under Contract F40600-69-C-0001 and ARO Project No. BB5822. Information in this report was prepared in partial fulfillment of the requirements for the degree of Master of Science. The manuscript was submitted for publication on July 25, 1969.

The author wishes to express his appreciation to Mr. F. C. Loper of Central Computer Operations of ARO, Inc., for his mathematical insight which led him to offer many suggestions and recommendations which were included in this study. Special thanks also are due to Mr. H. T. Bentley III of the staff research group of the technical staff of ARO, Inc., for his technical advice and his general support of this work.

This technical report has been reviewed and is approved.

Carlos Tirres
Captain, USAF
Research Division
Directorate of Plans
and Technology

Harry L. Maynard
Colonel, USAF
Director of Plans
and Technology

ABSTRACT

A numerical procedure is presented for the solution of the characteristic equations for a non-isoenergetic, supersonic, real gas jet expanding into a constant pressure ambience. Included is a procedure for inserting the expansion fan and the embedded shock. Examples are given for high temperature argon jets with radiation.

CONTENTS

ILLUSTRATIONS

NOMENCLATURE

A	Argon atom
a	Acoustic speed
BP	Upper field point
C_l	Constant
E_r	Energy of the rth specie
e	Electron
g_l	Degeneracy of the lth energy level
H	Stagnation enthalpy
h	Enthalpy
h	Planck's constant
I_r	Ionization energy of the rth specie relative to next lower level specie
K	Kelvin scale
k	Boltzmann's constant
M	Mach number
M_T	Total mass of mixture
m	Particle mass
N_l	Position on normal to oblique shock
N_r	Total number of particles of rth specie
n	Transformed coordinate normal to oblique shock
n_r	Number density of the rth specie
p	Pressure
Q	Flux of dissipating energy

Q_{rot}	Rotational partition function
Q_{trans}	Translational partition function
Q_{vib}	Vibrational partition function
r	Radial coordinate
s	Transformed coordinate tangent to oblique shock
SP1	Upstream shock point
SP2	Downstream shock point
T	Temperature
u	Axial component of velocity
V	Volume
VP	Virtual point
v	Radial component of velocity
w	Magnitude of velocity vector
X_l	Right hand side of various finite difference equations as defined in text
Z	Electronic partition function
z_i	Ionic charge
z	Axial coordinate
β	Oblique shock angle
ρ	Density
θ	Local flow angle
θ_r	Characteristic temperature of rth species

SUBSCRIPTS

A	Argon atom

e	Electron
I	General index
LI	Left running characteristic from point I
L2	Left running characteristic from point 2
RI	Right running characteristic from point I
R2	Right running characteristic from point 2
r	Specie or level of ionization
S.L.	Streamline

SUPERSCRIPTS WITH SUBSCRIPTS

$\bar{}$	Barred symbols are averages
$\bar{}_1$	Average of values at points I and 4
$\bar{}_2$	Average of values at points 2 and 4
$\bar{}_3$	Average of values at points 3 and 4

CHAPTER I
INTRODUCTION

I. PURPOSE

With the increased research emphasis on high temperature jets, the effects of radiation as well as real gas effects have taken on increased importance. Consequently the analytical tools, i.e. the mathematical models, for studying these jets need further development.

Available solutions make at least one if not all of the following assumptions: (1) the gas is perfect; (2) stagnation enthalpy is constant along streamlines; (3) the flow is irrotational; (4) embedded shocks can be neglected.

The purpose of this study, then, is to solve the system of characteristic equations obtained without any of these assumptions.

It is anticipated that the resulting computer program will be a valuable research tool.

II. PHYSICAL CONSIDERATIONS

When a supersonic jet exhausts into a lower pressure environment, a complex flow field is created as in Figure 1.

The fluid at the nozzle lip goes through an immediate expansion to the ambient pressure. Since in supersonic flow disturbances are propagated downstream only, the remainder of the fluid in the same plane as

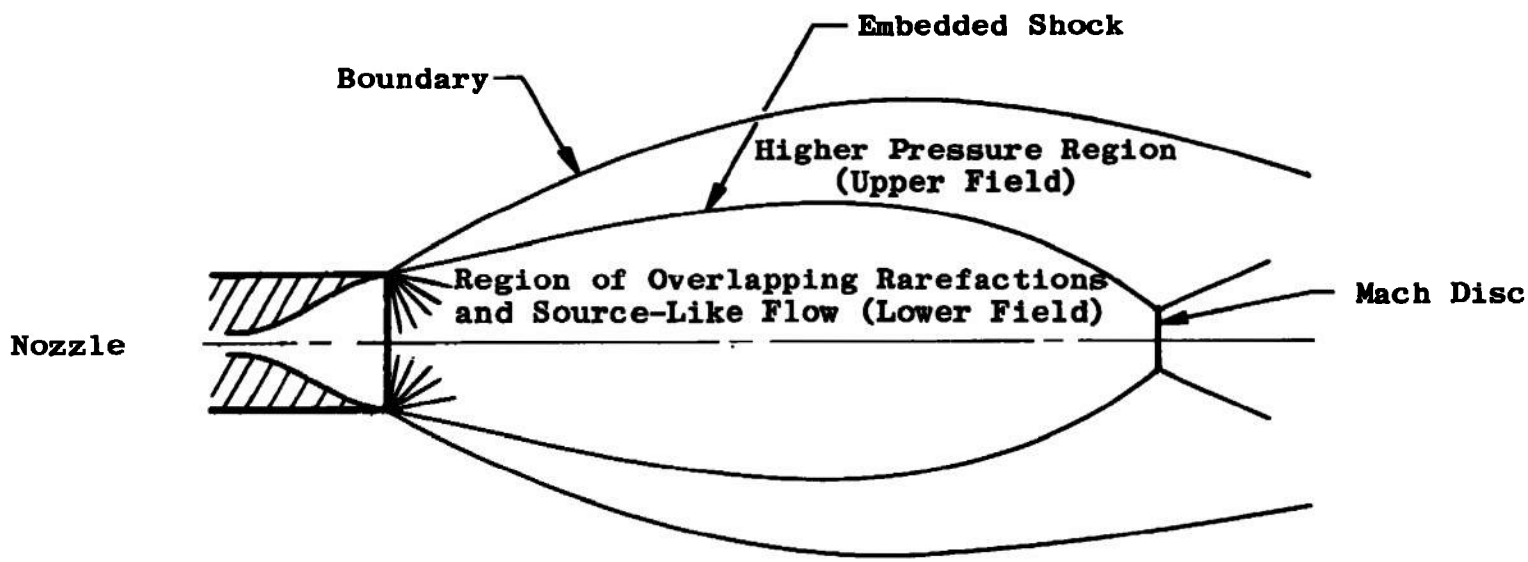

Fig. 1 Structure of Supersonic Field

the nozzle exit remains undisturbed. However, as the core of this jet encounters the rarefaction propagated from the nozzle lip, it too goes through an expansion. When the flow encounters the rarefaction propagated across the centerline from a point on the nozzle lip diametrically opposite, further expansion is induced such that a pressure much lower than ambient is reached. The flow must then recompress to the boundary pressure. Thus, a pressure trough could be said to form that deepens as the core of the flow encounters the overlapped rarefactions. While near the boundary, the pressure remains close to ambient. Until it encounters the higher pressure region near the boundary, the core is not influenced by whether it is expanding into a modest pressure difference or into a vacuum.

It is convenient to think of the field as consisting of two regions: an upper and a lower field. In the lower field occur the combined rarefactions causing the overexpansion. It is tempting to call this a source flow field as indeed it is assumed in Reference (1)[1]. That is, the flow appears to radiate from a point source.

At odds with this is the upper field which is at a higher pressure since it is influenced by disturbances from the boundary. Since the boundary of the flow is a streamline, the dominant direction of the upper field could be considered as being axial.

Obviously along some line in the plane being considered there

---

[1]Numbers in parentheses refer to similarly numbered references in the bibliography.

will be a conflict. On this line multiple conditions appear likely to occur. The flow will at once encounter a dominantly source-like, low pressure region and a mainly axial, higher pressure region.

An oblique shock serves to couple the two differing fields. This shock, variously named an embedded shock, boundary shock, secondary shock, barrel shock, and incident shock, starts as a weak shock emanating from the nozzle lip following the outer portion of the expansion fan. As the pressure trough deepens, the shock strengthens and finally curves toward the axis. The method of characteristics solution predicts the intersection of the shock with the axis if subsonic conditions are not encountered first. However, in actuality the phenomenon of the Mach disc occurs before then. The Mach disc is a normal shock behind which there is subsonic flow.

CHAPTER II
THEORY

I. DERIVATION OF CHARACTERISTIC EQUATIONS

The conservation equations are derived in most textbooks on theoretical gas dynamics. For an axially symmetric, inviscid, compressible, non-isoenergetic flow they are considered as:

for conservation of mass,

$$\rho v + r \frac{\partial \rho v}{\partial r} + r \frac{\partial \rho u}{\partial z} = 0 \tag{1}$$

for conservation of axial momentum,

$$\rho u \frac{\partial u}{\partial z} + \rho v \frac{\partial u}{\partial r} + \frac{\partial p}{\partial z} = 0 \tag{2}$$

for conservation of radial momentum,

$$\rho u \frac{\partial v}{\partial z} + \rho v \frac{\partial v}{\partial r} + \frac{\partial p}{\partial r} = 0 \tag{3}$$

and for the conservation of energy,

$$\rho u \frac{\partial H}{\partial z} + \rho v \frac{\partial H}{\partial r} = Q(z,r,u,v,p,h) \tag{4}$$

This is a set of four equations for the four unknowns u, v, p, and h since

$$H = \tfrac{1}{2}(u^2 + v^2) + h \tag{5}$$

and from the equation of state,

$$\rho = f(p,h) \tag{6}$$

Following Reference (2), Equations 1 to 4 are rewritten in a form such that only the dependent variables appear in the derivatives with respect to the coordinate variables. They become, using Equations 5 and 6,

$$\rho r \frac{\partial u}{\partial z} + \rho r \frac{\partial v}{\partial r} + ur \frac{\partial \rho}{\partial p}\frac{\partial p}{\partial z} + rv \frac{\partial \rho}{\partial p}\frac{\partial p}{\partial r} + ru \frac{\partial \rho}{\partial h}\frac{\partial h}{\partial z} + rv \frac{\partial \rho}{\partial h}\frac{\partial h}{\partial r} = -\rho v \tag{7}$$

$$\rho u \frac{\partial u}{\partial z} + \rho v \frac{\partial u}{\partial r} + \frac{\partial p}{\partial z} = 0 \tag{8}$$

$$\rho u \frac{\partial v}{\partial z} + \rho v \frac{\partial v}{\partial r} + \frac{\partial p}{\partial r} = 0 \tag{9}$$

$$\rho u^2 \frac{\partial u}{\partial z} + \rho uv \frac{\partial u}{\partial r} + \rho uv \frac{\partial v}{\partial z} + \rho v^2 \frac{\partial v}{\partial r} + \rho u \frac{\partial h}{\partial z} + \rho v \frac{\partial h}{\partial r} = Q \tag{10}$$

These four equations along with the definitions:

$$\frac{\partial u}{\partial z} dz + \frac{\partial u}{\partial r} dr = du \tag{11}$$

$$\frac{\partial v}{\partial z} dz + \frac{\partial v}{\partial r} dr = dv \tag{12}$$

$$\frac{\partial p}{\partial z} dz + \frac{\partial p}{\partial r} dr = dp \tag{13}$$

$$\frac{\partial h}{\partial z} dz + \frac{\partial h}{\partial r} dr = dh \tag{14}$$

are considered to be a linear system of eight algebraic equations and

eight unknowns. The unknowns are taken to be the partial derivatives of the dependent variables with respect to the independent variables.

The question is then asked, "Do curves exist within the domain of interest on which these derivatives may be discontinuous?"

It can be shown that these curves do exist if the function Q in Equation 10 is not a function of the derivatives of the dependent variables.

This involves a tedious expansion of large determinants which will not be presented here. The resulting equations are

$$udr - vdz = 0 \tag{15}$$

which is recognized as the equation of a streamline;

$$(u^2-a^2)dr^2 - 2uvdrdz + (v^2-a^2)dz^2 = 0 \tag{16}$$

where because of the choice of dependent variables

$$a^2 = \frac{\rho}{\frac{\partial \rho}{\partial h} + \rho \frac{\partial \rho}{\partial p}} \quad ; \tag{17}$$

and

$$\begin{aligned} &(udr-vdz)(udv-vdu) + (udr-vdz)^2 v/r \\ &+ \frac{dp}{\rho}(vdr+udz) + \frac{1}{\rho^2}\frac{\partial \rho}{\partial h}(udr-vdz)^2 Q = 0 \end{aligned} \tag{18}$$

which holds along the curves described by Equation 16;

also

$$dp/\rho + udu + vdv = 0 \tag{19}$$

which is Bernoulli's equation; and

$$dh + udu + vdv = Qdz/\rho u \tag{20}$$

which is recognized as the energy equation along a streamline.

The curves described by Equation 16 are referred to as the left or right running characteristics, while Equation 17 is simply the acoustic speed. Equations 18 to 20 are usually referred to as the compatibility relations.

From the original conservation equations, a rather remarkable set of relations has been obtained. These are relations for three families of curves along each of which is given the relationship among the flow properties in the form of ordinary differential equations.

These equations are put in finite difference form and solved numerically. The detailed procedure is presented in Chapter III.

II. EXPANSION AT THE NOZZLE LIP

At the nozzle lip the flow must turn abruptly to match the ambient pressure. In an inviscid flow, the flow properties are not single valued, i.e. the field at that point is assumed to experience a continuous change in pressure from the pressure existing at the nozzle exit to the ambient pressure. A relation, then, is needed for the properties at a point as a function of pressure.

This relation, the so called Prandtl-Meyer relation, can be derived in many ways. It is interesting to see that it can be obtained readily from the compatibility relations.

Dividing Equation 18 through by udr-vdz and taking the limit as dr and dz go to zero along a left running characteristic, the expression

$$\lim_{\substack{dr \to 0 \\ dz \to 0}} \left\{ udv - vdu + (udr - vdz)\frac{v}{r} + \frac{dp}{\rho}\left[\frac{vdr + udz}{udr - vdz}\right] + \frac{1}{\rho^2}\frac{\partial \rho}{\partial h}(udr - vdz)Q \right\} = 0$$

becomes

$$udv - vdu + \frac{dp}{\rho}\left\{\lim_{\substack{dr \to 0 \\ dz \to 0}} \left[\frac{vdr + udz}{udr - vdz}\right]\right\} = 0 \tag{21}$$

By taking the limit along the path, the slope of which is given by Equation 16, i.e.

$$\frac{dr}{dz} = \frac{uv + a\sqrt{u^2 - a^2 + v^2}}{u^2 - a^2} \tag{22}$$

Equation 21 becomes

$$udv - vdu + \frac{dp}{\rho}\left\{\sqrt{M^2 - 1}\right\} = 0 \tag{23}$$

where

$$M^2 = \frac{u^2 + v^2}{a^2}$$

Also, the limit of the compatibility relations along a streamline is taken, obtaining

$$udu + vdv = -\frac{dp}{\rho} \tag{24}$$

and

$$dh + udu + vdv = 0 \tag{25}$$

Equation 25 is integrated directly giving

$$h + \frac{u^2 + v^2}{2} = \text{constant} \tag{26}$$

Equations 23 and 24 are then arranged such that

$$u\frac{dv}{dp} - v\frac{du}{dp} = -\frac{\sqrt{M^2 - 1}}{\rho}$$

$$v\frac{dv}{dp} + u\frac{du}{dp} = -\frac{1}{\rho}$$

Using Cramer's rule

$$\frac{du}{dp} = \frac{-\frac{u}{\rho} + v\frac{\sqrt{M^2 - 1}}{\rho}}{u^2 + v^2} \tag{27}$$

and

$$\frac{dv}{dp} = \frac{-\frac{u}{\rho}\sqrt{M^2 - 1} - \frac{v}{\rho}}{u^2 + v^2} \tag{28}$$

Equations 27 and 28 can be written more familiarly in polar form for the velocity as

$$\frac{d\theta}{dp} = - \frac{\sqrt{M^2 - 1}}{\rho w^2} \tag{29}$$

and

$$\frac{dw}{dp} = - \frac{1}{\rho w} \tag{30}$$

Thus, with Equations 26, 27, and 28, the variables u, v, and h can be determined as a function of p. Consequently, the properties at a point on the nozzle lip are determined by varying pressure between its initial value and the boundary value and solving for u, v, and h.

III. EMBEDDED SHOCK

As discussed in the introduction, an embedded or secondary shock is encountered in the flow field. In the physical field the shock occurs when the Mach waves coalesce. The shock wave occurs in the solution field when characteristic curves of the same sense, say right-running, coalesce and finally overlap one another. This is treated as a discontinuity in the dependent variables. To cross the discontinuity the oblique shock relations must be utilized.

The shock relations follow from the conservation equations, Equations 1, 2, 3, and 4. Consider, for example, the energy equation. Multiplying the continuity equation by H and adding it to the energy equation gives

$$\frac{\partial(\rho u H)}{\partial z} + \frac{\partial(\rho v H)}{\partial r} = Q - \frac{\rho v H}{r} \tag{30}$$

Now, consider the surface of discontinuity of the dependent variables as occurring at an angle β, Figure 2, with the axial coordinate at the point of interest in the r-z plane. Transforming Equation 30 in the r-z plane to coordinate normal and tangent to the curve, say n and s, Equation 30 then becomes

$$\frac{\partial(\rho uH)}{\partial n} \sin\beta + \frac{\partial(\rho uH)}{\partial s} \cos\beta + \frac{\partial(\rho vH)}{\partial n} \cos\beta - \frac{\partial(\rho vH)}{\partial s} \sin\beta = Q - \frac{\rho vH}{r} \tag{31}$$

Adding terms to both sides to complete the derivative gives

$$\frac{\partial}{\partial n} (\rho uH \sin\beta + \rho vH \cos\beta) + \frac{\partial}{\partial s} (\rho uH \cos\beta - \rho uH \sin\beta) = Q - \frac{d\beta}{ds} (\rho vH \cos\beta + \rho uH \sin\beta) - \frac{\rho vH}{r} \tag{32}$$

Taking the integral of both sides with respect to n gives

$$\int_{N_1}^{N_2} \frac{\partial}{\partial n} (\rho uH \sin\beta + \rho vH \cos\beta)\, dn + \int_{N_1}^{N_2} \frac{\partial}{\partial s} (\rho uH \cos\beta - \rho vH \sin\beta)\, dn = \int_{N_1}^{N_2} Q\, dn - \int_{N_1}^{N_2} (\rho vH \cos\beta + \rho uH \sin\beta) \frac{d\beta}{ds}\, dn - \int_{N_1}^{N_2} \frac{\rho vH}{r}\, dn \tag{33}$$

Assuming the existence of the integrals and the continuity of the integrand of the first integral on the left hand side for all $N_1 \leq n \leq N_2$,

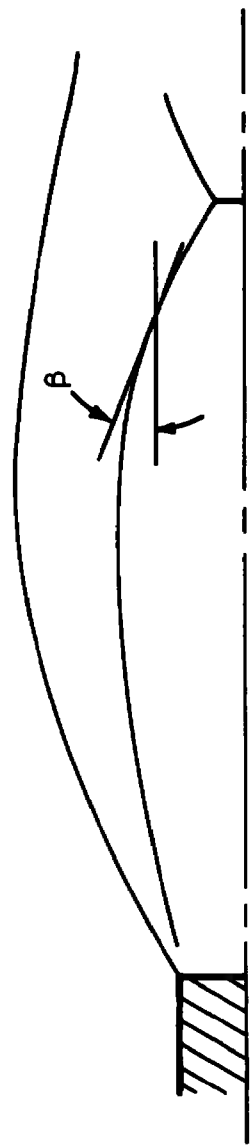

Fig. 2 Local Angle of Embedded Shock

$$(\rho uH \sin \beta + \rho vH \cos \beta)\Big|_{N_2} - (\rho uH \sin \beta + \rho vH \cos \beta)\Big|_{N_1}$$

$$+\int_{N_1}^{N_2} \frac{\partial}{\partial s} (\rho uH \cos \beta - \rho vH \sin \beta) dn = \int_{N_1}^{N_2} Q dn$$

$$-\int_{N_1}^{N_2} (\rho vH \cos \beta + \rho uH \sin \beta) \frac{d\beta}{ds} dn - \int_{N_1}^{N_2} \frac{\rho vH}{r} dn \qquad (34)$$

The integrals then vanish in the limit as N_2 and N_1 are made to approach a point on the discontinuity from opposite sides, or

$$\rho_2 u_2 H_2 \sin \beta + \rho_2 v_2 H_2 \cos \beta = \rho_1 u_1 H_1 \sin \beta + \rho_1 v_1 H_1 \cos \beta \qquad (35)$$

A similar procedure on the mass and momentum equation yields

$$\rho_2 u_2 \sin \beta + \rho_2 v_2 \cos \beta = c_1 \qquad (36)$$

$$\rho_2 u_2 \sin \beta + \rho_2 v_2 \cos \beta\, u_2 + p_2 \sin \beta = c_2 \qquad (37)$$

$$\rho_2 u_2 \sin \beta\, v_2 + \rho_2 v_2 \cos \beta\, v_2 + p_2 \cos \beta = c_3 \qquad (38)$$

and Equation 35 may be written as

$$\rho_2 u_2 \sin \beta\, h_2 + \rho_2 v_2 \cos \beta\, h_2 + \rho_2 u_2 \sin \beta \frac{u_2^2}{2}$$

$$+ \rho_2 v_2 \cos \beta \frac{u_2^2}{2} + \rho_2 u_2 \sin \beta \frac{v_2^2}{2} + \rho_2 v_2 \cos \beta \frac{v_2^2}{2} = c_4 \qquad (39)$$

where the c values are known from upstream properties. More simply

$$\rho_2 u_2 \sin \beta + \rho_2 v_2 \cos \beta = c_1 \tag{40}$$

$$c_1 u_2 + p_2 \sin \beta = c_2 \tag{41}$$

$$c_1 v_2 + p_2 \cos \beta = c_3 \tag{42}$$

and

$$h_2 + \frac{u_2^2}{2} + \frac{v_2^2}{2} = \frac{c_4}{c_1} \tag{43}$$

This is a set of four non-linear algebraic equations which were solved for the downstream properties u_2, v_2, p_2, and h_2, the density being determined from the thermal equation of state.

IV. DISSIPATION MODEL

Energy loss from a high temperature jet is chiefly through the mechanisms of conduction and radiation. The dissipation term required for the right hand side of Equation 20 is one in which no derivatives of the dependent variables appear. The usual conduction term, therefore, cannot be utilized. However, there are several radiation models that fulfill this requirement.

In general, radiation from high temperature plasmas is considered to be the continuum due to free-free and free-bound transitions of the electrons. However, free-bound radiation occurs only where there is recombination, which occurs when the flow is near equilibrium.

At pressures in the range of 0.01 and 0.5 atmospheres, it is not uncommon to consider the flow as frozen to recombination. Even if

the flow is nearer to equilibrium at the higher pressures, it reduces computation considerably to assume frozen flow. This allows the investigator to study trends and the effects of various parameters on the flow with but a fraction of the computer time.

Assuming the flow frozen to recombination, the radiation would be due to free-free interactions. Reference (3) gives a relation due to Spitzer for a fully ionized argon gas with free-free radiation only as

$$Q = - 1.569 \times 10^{-34} n_e \sum_i n_i (z_i)^2 T^{\frac{1}{2}} \quad w\text{-}cm^{-3} \tag{44}$$

However, this relation gives smaller values than those measured by References (4) and (5). Multiplying this relation by 15 gives a better approximation to these results.

Regardless of whether this approximation is good or bad, and there is enough confusion in the literature to suggest that it is as good as any, it serves to illustrate the use of the solution.

V. GAS MODEL

Following Reference (6), for an ionized gas consider the reaction

$$A_r \rightleftharpoons A_{r+1} + e \tag{45}$$

where A_r is an ionized particle and A_{r+1} is the next higher ionized particle. The equilibrium constant for the reaction can be expressed as

$$\frac{n_{r+1}\, n_e}{n_r} = \left(\frac{2\pi\, m_e kT}{h^2}\right)^{3/2} \frac{2\, Z_{r+1}}{Z_r} \exp\left(-\frac{\theta_r}{T}\right) \tag{46}$$

Here Z_r is the electronic partition function corresponding to particle A_r, and Z_{r+1} is the partition function for the next higher ionization. The parameter θ_r is the characteristic temperature for ionization. As the gas is assumed to be a mixture of perfect gases, the equation of state may be written for three levels of ionization as

$$\frac{p}{kT} = n_o + n_1 + n_2 + n_3 + n_e \tag{47}$$

and the conservation of charge is stated as

$$n_e = n_1 + 2n_2 + 3n_3 \tag{48}$$

Equations 46, 47, and 48 are a system of five non-linear equations with five unknowns which were solved for the particle densities. Thus given P and T, density is returned as

$$\rho = m_A (n_o + n_1 + n_2 + n_3) \tag{49}$$

The energy of a particle is divided among its translational, rotational, vibrational, and electronic modes (see Reference (7)). This energy depends on the partition function for each mode. In general,

$$\frac{E_r}{N_r} = kT^2 \frac{\partial(\ell n Q_r)}{\partial T} + I_r \tag{50}$$

where E_r is the total energy for a particular species, I_r is the

ionization energy per particle, and N_r is the total number of particles present, and

$$Q = Q_{trans.} \times Q_{rot} \times Q_{vib} \times Z \tag{51}$$

For a monatomic gas, the rotational and vibrational modes are not present. Therefore, $Q_{rot} = Q_{vib} = 1$, and

$$\frac{E_r}{N_r} = kT^2 \left[\frac{\partial(\ell n\, Q_{trans.})}{\partial T} + \frac{\partial(\ell n\, Z_r)}{\partial T} \right] + I_r$$

From statistical mechanics,

$$Q_{trans.} = V \left(\frac{2\pi mkT}{h^2} \right)^{3/2}$$

and

$$Z_r = [g_o + g_1\, e^{-\theta_1/T} + g_2\, e^{-\theta_2/T} + \ldots]_r$$

where θ_1, θ_2 ... , are the characteristic temperatures for electronic excitation. The symbols g_o, g_1, ... etc., represent the degeneracy factors of the energy levels of the atomic structure. Specifically for a monatomic gas

$$g_i = 2J_i + 1$$

where J_i are the inner quantum numbers as given in Reference (8). Equation 50 then becomes

$$\frac{E_r}{N_r} = \frac{3}{2} kT + \frac{k\left[g_1\theta_1 e^{-\theta_1/T} + g_2\theta_2\, e^{-\theta_2/T} + \ldots\right]_r}{\left[g_o + g_1 e^{-\theta_1/T} + g_2 e^{-\theta_2/T} + \ldots\right]_r} + I_r \tag{52}$$

Since for a particular species

$$p_r V = N_r kT$$

and the enthalpy is defined as

$$H_r = E_r + p_r V$$

The "enthalpy per particle" becomes

$$\frac{H_r}{N_r} = \frac{5}{2} kT + \frac{k\left[g_1\theta_1 e^{-\theta_1/T} + g_2\theta_2 e^{-\theta_2/T} + \ldots \right]_r}{Z_r} + I_r$$

The contribution of this specie to the specific enthalpy of the mixture is

$$h_r = \frac{N_r}{M_T} \left[\frac{5}{2} kT + \frac{k \sum_i \theta_{r,i}\, g_{r,i}\, e^{-\theta_{r,i}/T}}{Z_r} + I_r \right]$$

where M_T is the total mass of the mixture. By summing over the several species, the enthalpy of the mixture becomes

$$h = \frac{1}{\rho} \sum_{o}^{3} n_r \left[\frac{5}{2} kT + kT^2 \frac{Z_r'}{Z_r} + I_r \right] + \frac{1}{\rho} n_e \frac{5}{2} kT \qquad (53)$$

where

$Z_e' = I_e = 0$ for electrons.

VI. MACH DISC

The location of the so called Mach disc is important to many observers as its attendant subsonic region cannot be analyzed by the

characteristics method. Also, the method of characteristics cannot predict the location of the disc, i.e. the location of the embedded oblique shock is determined until it intersects the axis. The Mach disc occurs at some point before the intersection.

Several methods have been offered to determine the Mach disc location. A review of these methods is presented in Reference (9). A method suggested by Eastman and Radtke (10), is simple and according to Reference (9) is reasonably accurate for plume exhausting into still air. They hypothesize that the Mach disc occurs at the point where the static pressure behind the oblique shock reaches a minimum. They give no reason other than observation to support their contention. Nevertheless, their predictions fall relatively close to other more sophisticated predictions.

CHAPTER III
NUMERICAL PROCEDURES

I. INTRODUCTION

In this chapter the method of characteristics will be formulated for machine computation. The choice of procedure is largely subjective, and the efficiency of one procedure over another is not readily apparent.

II. GENERAL CONSIDERATIONS

As the solution of the characteristic equations is an initial value problem, the flow properties along some starting line must be known. That is, at each point u, v, p, and h must be specified. Arbitrarily, the starting line is chosen to be the exit plane of the nozzle.

The computation begins at the starting line point on the nozzle lip as in Figure 3. The nozzle exit pressure and the ambient pressure exist at this point. Using pressure as an independent variable, the Prandtl-Meyer relations are used to compute a set of properties for the point for each arbitrary increment in pressure from the exit pressure to the ambient pressure. The next point down on the starting line is used in conjunction with the nozzle lip point to compute a third point downstream. The nozzle lip point is treated as though its properties were

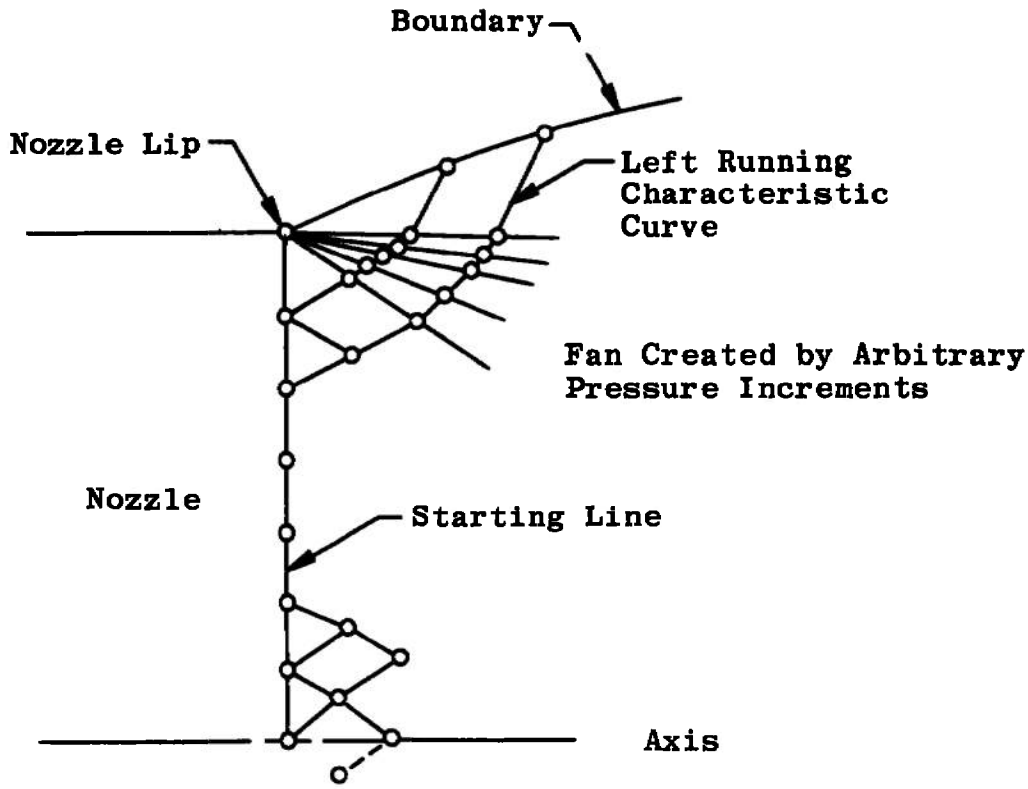

Fig. 3 Typical Expansion Network

those existing at the nozzle exit.

Using this new point and the nozzle point with properties resulting from its first pressure increment, a fourth point and its attendant properties are computed. As each point is obtained, its properties are stored in the computer for further use. When the boundary is encountered, i.e. the pressure matches the boundary pressure, its properties are computed and stored. This storage array then fully defines a complete left-running characteristic curve. Using the next point on the starting line and the points just computed, a new left-running characteristic is computed, and so on until the starting line point on the axis has been used. The next characteristic begins from an axis point downstream from the starting line. It is computed using the method of reflection, whereby a point in the upper half plane is "reflected" in the lower half plane. The original point and its "image" are used to compute the point on the axis.

The computation continues until a point is computed that is closer to the beginning of a left-running characteristic than the previous point. This indicates that a "fold back" is occurring. At this point the oblique shock wave is considered to begin.

As in Chapter I, the field above the point of foldback is considered the upper field and the field below, the lower field. The field properties within the foldback are doubly defined. Guessing a possible shock angle, using the properties of the point as defined by the lower field, and substituting into the oblique shock relations, a set of flow properties result that should match the properties of the point

as defined by the upper field. If there is no match, another shock angle must be assumed, and so on until a matching has occurred.

The computation then proceeds as before except that two sets of flow properties are stored for each shock point. The computation is self-terminating when the shock intercepts the axis or when the shock becomes so strong that the downstream flow becomes subsonic.

III. TYPICAL FIELD POINT CALCULATION

In Figure 4 the position and flow properties of points 1 and 2 are known either from previous computation or from initial conditions.

Putting Equations 15, 18, 19, 20, and 22 in finite difference form,

$$\left(\frac{\Delta r}{\Delta z}\right)_{S.L.} = \frac{\bar{v}_3}{\bar{u}_3} \tag{54}$$

$$\left(\frac{\Delta r}{\Delta z}\right)_{L1} = \frac{\bar{u}_1\bar{v}_1 + \bar{a}_1\sqrt{\bar{u}_1^2 - \bar{a}_1^2 + \bar{v}_1^2}}{\bar{u}_1^2 \ominus \bar{a}_1^2} \tag{55}$$

$$\left(\frac{\Delta r}{\Delta z}\right)_{R2} = \frac{\bar{u}_2\bar{v}_2 - \bar{a}_2\sqrt{\bar{u}_2^2 - \bar{a}_2^2 + \bar{v}_2^2}}{\bar{u}_2^2 \ominus \bar{a}_2^2} \tag{56}$$

$$\left[\bar{u}_1\left(\frac{\Delta r}{\Delta z}\right)_{L1} - \bar{v}_1\right]\bar{u}_1 v_4 - \left[\bar{u}_1\left(\frac{\Delta r}{\Delta z}\right)_{L1} - \bar{v}_1\right]\bar{v}_1 u_4 + \frac{1}{\bar{\rho}_1}\left[\bar{v}_1\left(\frac{\Delta r}{\Delta z}\right)_{L1} + \bar{u}_1\right]p_4 = X_1 \tag{57}$$

$$\left[\bar{u}_2\left(\frac{\Delta r}{\Delta z}\right)_{R2} - \bar{v}_2\right]\bar{u}_2 v_4 - \left[\bar{u}_2\left(\frac{\Delta r}{\Delta z}\right)_{R2} - \bar{v}_2\right]\bar{v}_2 u_4 + \frac{1}{\bar{\rho}_2}\left[\bar{v}_2\left(\frac{\Delta r}{\Delta z}\right)_{R2} + \bar{u}_2\right]p_4 = X_2 \tag{58}$$

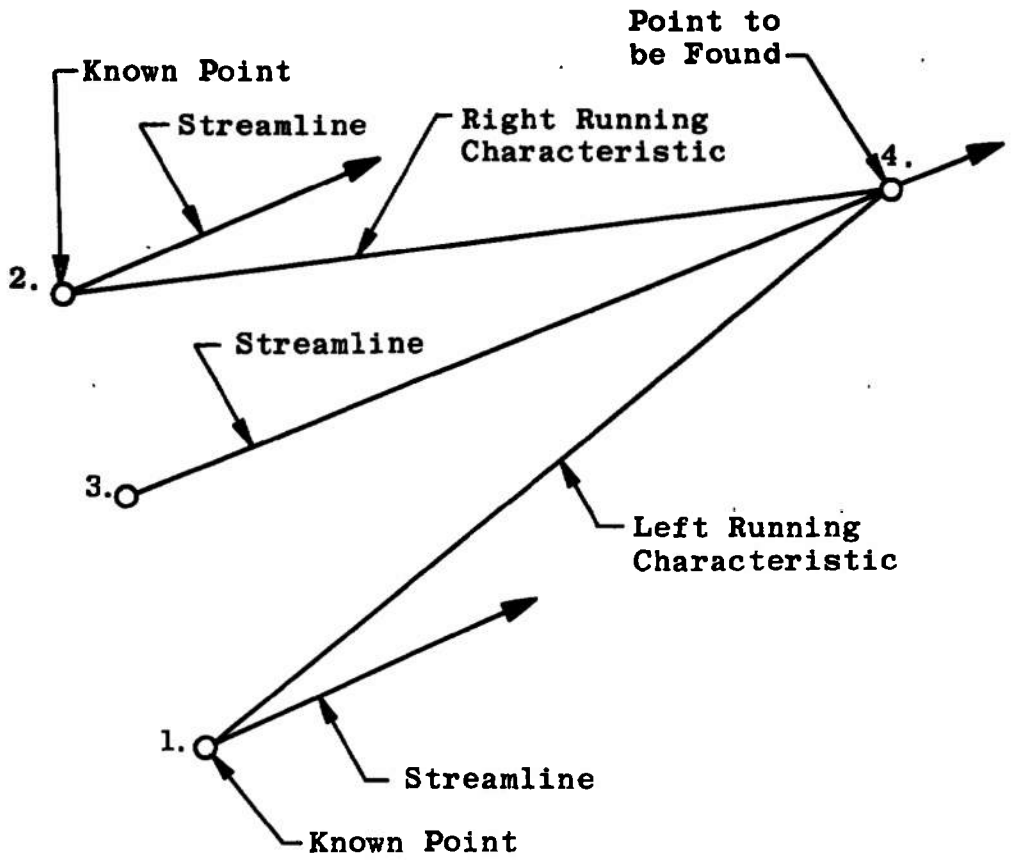

Fig. 4 Locating of Third Point from Two Known Points

and

$$\bar{\rho}_3\bar{v}_3v_4 + \bar{\rho}_3\bar{u}_3u_4 + p_4 = X_3 \tag{59}$$

$$\bar{v}_3v_4 + \bar{u}_3u_4 + h_4 = X_4 \tag{60}$$

where

$$X_1 = -\left[\bar{u}_1\left(\frac{\Delta r}{\Delta z}\right)_{L1} - \bar{v}_1\right]^2 \frac{\bar{v}_1}{\bar{r}_1}(Z_4-Z_1) + \frac{1}{\bar{\rho}_1}\left[\bar{v}_1\left(\frac{\Delta r}{\Delta z}\right)_{L1} + \bar{u}_1\right]p_1$$

$$+ \left[\bar{u}_1\left(\frac{\Delta r}{\Delta z}\right)_{L1} - \bar{v}_1\right]\bar{u}_1v_1 + \left[\bar{u}_1\left(\frac{\Delta r}{\Delta z}\right)_{L1} - \bar{v}_1\right]\bar{v}_1u_1$$

$$- \frac{1}{\bar{\rho}_1^2}\frac{\overline{\partial\rho_1}}{\partial h_1}\bar{Q}_1\left[\bar{u}_1\left(\frac{\Delta r}{\Delta z}\right)_{L1} - \bar{v}_1\right]^2 (Z_4-Z_1)$$

$$X_2 = -\left[\bar{u}_2\left(\frac{\Delta r}{\Delta z}\right)_{R2} - \bar{v}_2\right]^2 \frac{\bar{v}_2}{\bar{r}_2}(Z_4-Z_2) + \frac{1}{\bar{\rho}_2}\left[\bar{v}_2\left(\frac{\Delta r}{\Delta z}\right)_{R2} + \bar{u}_2\right]p_2$$

$$+ \left[\bar{u}_2\left(\frac{\Delta r}{\Delta z}\right)_{R2} - \bar{v}_2\right]\bar{u}_2v_2 + \left[\bar{u}_2\left(\frac{\Delta r}{\Delta z}\right)_{R2} - \bar{v}_2\right]\bar{v}_2u_2$$

$$- \frac{1}{\bar{\rho}^2}\frac{\overline{\partial\rho_2}}{\partial h_2}\bar{Q}_2\left[\bar{u}_2\left(\frac{\Delta r}{\Delta z}\right)_{R2} - \bar{v}_2\right]^2 (Z_4-Z_2)$$

$$X_3 = p_3 + \bar{\rho}_3\bar{v}_3v_3 + \bar{\rho}_3\bar{u}_3u_3$$

and

$$X_4 = (1/\bar{\rho}_3\bar{u}_3)\bar{Q}_3(Z_4-Z_3) + h_3 + \bar{v}_3v_3 + \bar{u}_3u_3$$

Equations 55$_1$ and 56 are used to find the tentative position of point 4. Except for $\bar{r}$, the barred values are initially taken to be the values at points 1 and 2. The $\bar{r}$ values are averages of the radial position of points 1 or 2 with the tentative radial position of point 4, i.e. $\bar{r}_1 = \frac{1}{2}(r_1+r_4)$. The streamline through points 3 and 4 is initially assumed to have the average slope of the streamlines through points 1 and 2. This slope and the position of point 4 initially determines the position of point 3. The properties of point 3 are determined by linear interpolation between points 1 and 2. Equations 57 to 60 along with the equation of state constitute a set of linear algebraic equations that are solved for the properties of point 4.

The barred symbols are now assigned the values of the average of the properties of the points 1 and 4, 2 and 4, and 3 and 4, i.e.,

$$\bar{u}_1 = \tfrac{1}{2}(u_1 + u_4)$$

$$\bar{u}_3 = \tfrac{1}{2}(u_3 + u_4)$$

$$\bar{u}_2 = \tfrac{1}{2}(u_2 + u_4)$$

and so on.

The position of point 4 is computed again. The slope of the streamline is now computed from Equation 54.

The position of point 3 is again determined in the same manner, and the set of equations is solved once more. This iteration is continued until consecutive values of the properties of point 4 agree within some allowable error.

IV. TYPICAL PRANDTL-MEYER EXPANSION

Consider Figure 5. Multiple sets of properties are assumed to exist at point 2, the point on the nozzle lip. The pressure is allowed to vary continuously from its value at the nozzle exit to the ambient pressure. The expansion fan is constructed in the following manner.

Point 4 is computed as a typical field point using the properties as given on the starting line.

Before computing point 4', however, the Prandtl-Meyer relations, Equations 27 and 28 along with Equation 26 must be used.

The pressure differential between the ambient pressure and the nozzle exit pressure is arbitrarily broken into several increments depending on network size desired. Using some integrating technique such as Runge-Kutta, Equations 27 and 28 are integrated over a pressure increment, determining the new velocity at point 2. Equation 26 yields the enthalpy directly. Using these new properties for point 2 and the properties of point 4, point 4' is readily determined as a typical field point calculation.

This procedure is continued until the ambient pressure is reached at point 2. The boundary point is then computed as a typical boundary point.

V. TYPICAL BOUNDARY POINT CALCULATION

Figure 6 could be considered as "half" of Figure 4, page 25. That is to say, since the boundary is formed by the streamline, the

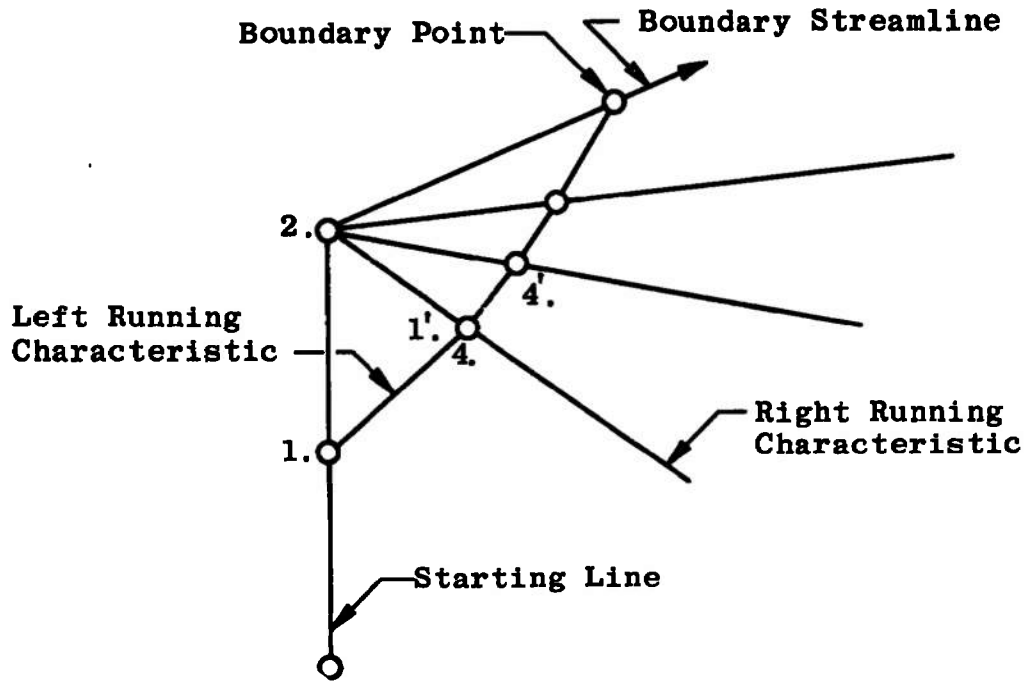

Fig. 5 Typical Expansion Fan Construction

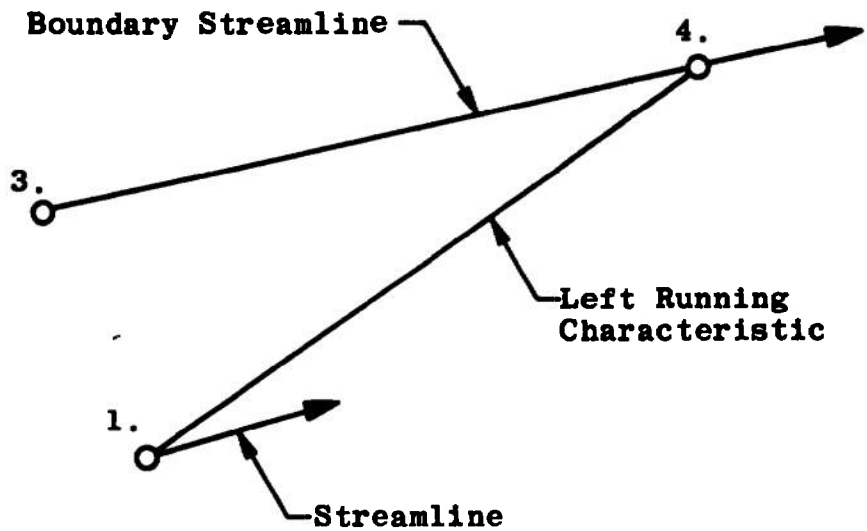

Fig. 6 Locating of Second Boundary Point from a Previously Known Boundary Point and Field Point

characteristic line between points 2 and 4 in Figure 4, page 25, lies outside the region of interest. Two boundary conditions replace the two relations defining this characteristic line and its properties.

One condition is simply that the boundary is a streamline. The second condition is that for a pressure boundary, the pressure is specified at all points along the boundary streamline, i.e.

$$p = f(z,r,u,v,h)$$

For the case considered here, the boundary is a free pressure boundary, i.e.

$$p = \text{constant}$$

The required difference relations are

$$\left(\frac{\Delta r}{\Delta z}\right)_{S.L.} = \frac{\bar{v}_3}{\bar{u}_3} \tag{61}$$

$$\left(\frac{\Delta r}{\Delta z}\right)_{LI} = \frac{\bar{u}_1\bar{v}_1 + \bar{a}_1\sqrt{\bar{u}_1^2 + \bar{v}_1^2 - \bar{a}_1^2}}{\bar{u}_1^2 \ominus \bar{a}_1^2} \tag{62}$$

$$\left[u_1\left(\frac{\Delta r}{\Delta z}\right)_{LI} - \bar{v}_1\right]\bar{u}_1 v_4 - \left[\bar{u}_1\left(\frac{\Delta r}{\Delta z}\right)_{LI} - \bar{v}_1\right]\bar{v}_1 u_4 = X_{BI} \tag{63}$$

$$\bar{\rho}_3\bar{v}_3 v_4 + \bar{\rho}_3\bar{u}_3 u_4 = \bar{\rho}_1\bar{v}_1 v_3 + \bar{\rho}_3\bar{u}_3 u_1 \tag{64}$$

and

$$\bar{v}_3 v_4 + \bar{u}_3 u_4 + h_4 = X_{B3} \tag{65}$$

where

$$X_{B1} = X_1 - \frac{1}{\bar{\rho}_1}\left[\bar{v}_1 \left(\frac{\Delta r}{\Delta z}\right)_{L1} + \bar{u}_1\right] p_4$$

and

$$X_{B3} = X_4$$

The expressions for X_1 and X_4 are unchanged from those in the typical field point calculation.

The solution procedure is similar to that of the typical field point, except that point 3 is fixed. Point 4 is tentatively found from Equations 61 and 62, then the linear set, Equations 63 to 65, are solved for the properties at point 4. New barred values are assigned, and so on following an iterative procedure.

VI. TYPICAL POINT ON THE AXIS

This being an axially symmetric problem, the calculation of axial points is quite simple using the method of reflection. From Figure 7, point 1 is reflected in the lower half plane as point 2, i.e.

$$z_2 = z_1$$

$$r_2 = - r_1$$

$$u_2 = u_1$$

$$v_2 = - v_1$$

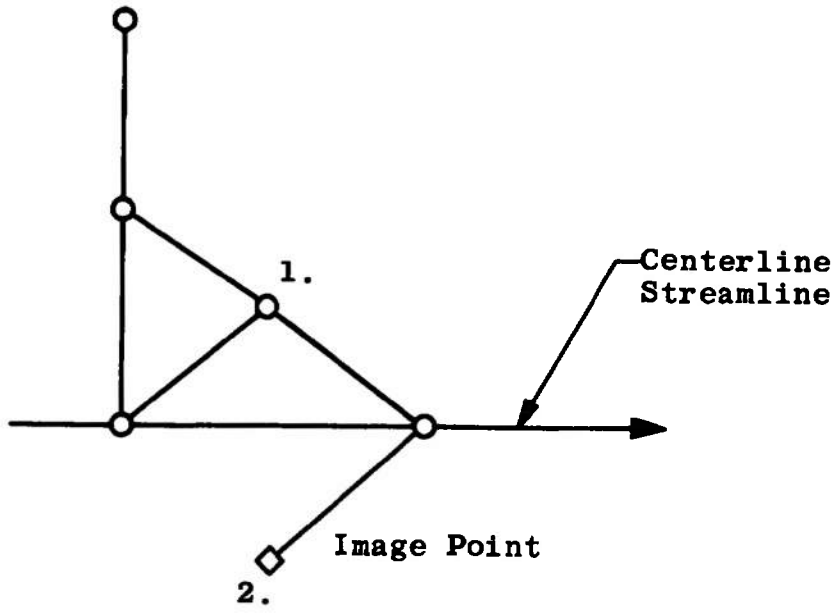

Fig. 7 Locating of Point on Axis Using Reflected Point

$$p_2 = p_1$$

and

$$h_2 = h_1$$

The calculation procedure is then that of a typical field point.

VII. TYPICAL SHOCK POINT

The starting of the interior shock is signaled when the condition depicted in Figure 8 occurs, i.e. when point 4 falls behind point 1, meaning that two right-running characteristics have crossed. Following Reference (11), the left-running characteristic curve B is completed to the boundary and point 4 is deleted from the field. Characteristic curve C is then completed up to the virtual point (point VP). Point 1 is considered as the first shock point.

A guess of the shock angle β is made such that the tentative shock line falls to the right of the characteristic line between points 1 and VP. Guessing β such that the shock line fell to the left results in an incorrect solution, i.e. no solution of the oblique shock relations can be found that has an entropy increase. This is because the limits of a shock angle are between that of a Mach line, here a characteristic, and a shock normal to the upstream flow.

The intersection of the shock line with characteristic C is found and its properties obtained by interpolation. These properties are the upstream properties at the shock point (point SP1).

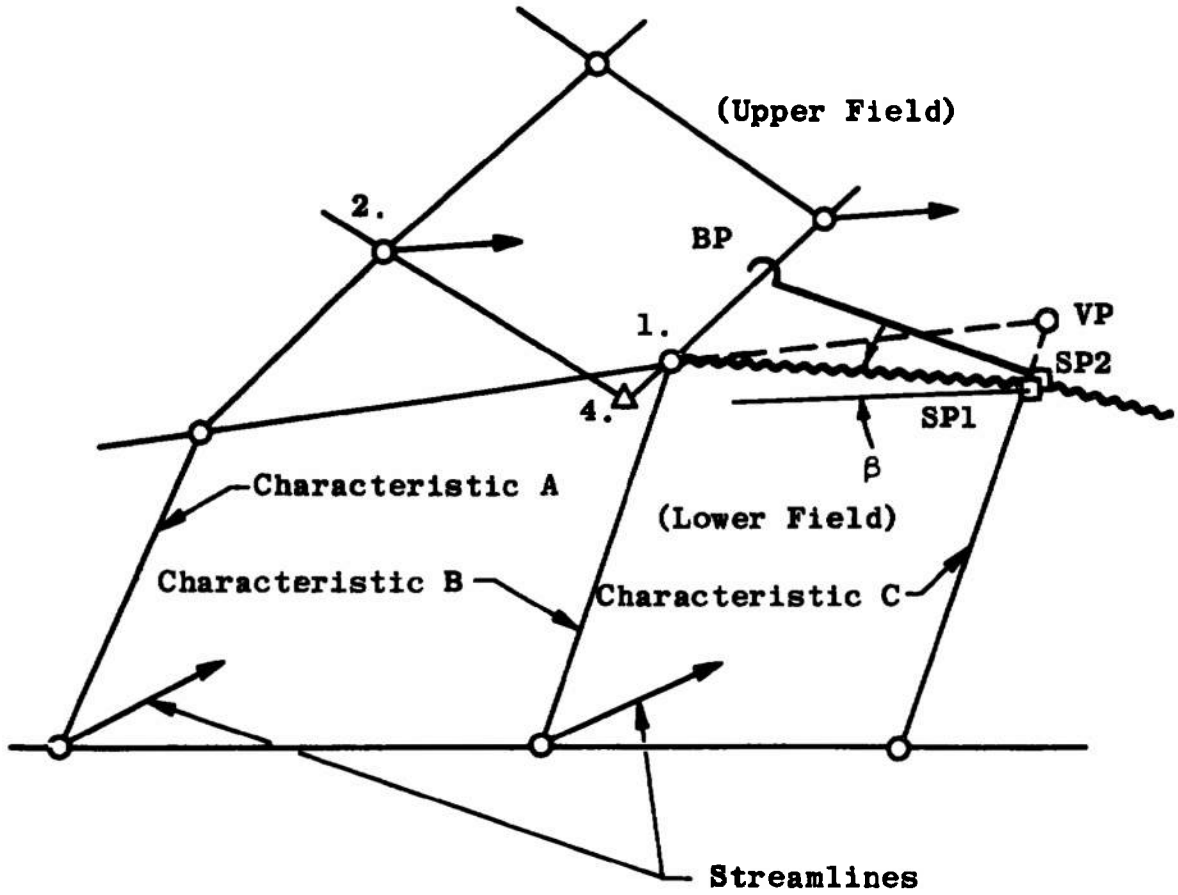

Fig. 8 Matching of Upper Field to Lower Field Through A Shock Point

The shock relations,

$$\rho_2 u_2 \sin\beta + \rho_2 v_2 \cos\beta = \rho_1 u_1 \sin\beta + \rho_1 v_1 \cos\beta = c_1$$

$$c_1 u_2 + p_2 \sin\beta = c_1 u_1 + p_1 \sin\beta$$

$$c_1 v_2 + p_2 \cos\beta = c_1 v_1 + p_1 \cos\beta$$

and

$$h_2 + \frac{u_2^2 + v_2^2}{2} = h_1 + \frac{u_1^2 + v_1^2}{2}$$

are then solved for the downstream properties at point SP2. (Note that points SP1 and SP2 have the same position.) The constants are, of course, determined from the upstream properties, while the subscript (2) here refers to downstream properties.

For this to be a solution, these properties must match those predicted by the upper field for this position.

First, construct a right-running characteristic through point SP2 to some point BP. The tentative slope is given by

$$\frac{\Delta r}{\Delta z} = \frac{\bar{u}\,\bar{v} - \bar{a}\sqrt{\bar{u}^2 - \bar{a}^2 + \bar{v}^2}}{\bar{u}^2 \ominus \bar{a}^2}$$

where the barred quantities are initially assigned the values of the properties at point SP2. The tentative point BP is found and its properties interpolated for in characteristic B. The barred values are then assigned the value of the average properties of points SP2 and BP. A new slope is found and then a new position, and so on. The iteration is stopped when succeeding positions of point BP change less

than some allowable error. The barred values and the delta values are then substituted into the finite difference form of the compatibility relation for a right-running characteristic, i.e.

$$\left[\bar{u}\left(\frac{\Delta r}{\Delta z}\right) - \bar{v}\right]\bar{u}\,\Delta v - \left[\bar{u}\left(\frac{\Delta r}{\Delta z}\right) - \bar{v}\right]\bar{v}\,\Delta u + \frac{1}{\bar{\rho}}\left[\bar{v}\left(\frac{\Delta r}{\Delta z}\right) + \bar{u}\right]\Delta p$$

$$+\left[\bar{u}\left(\frac{\Delta r}{\Delta z}\right) - \bar{v}\right]^2 \frac{\bar{v}}{\bar{r}}\,\Delta z + \frac{1}{\bar{\rho}^2}\,\overline{\frac{\partial \rho}{\partial h}}\,\bar{Q}\left[\bar{u}\left(\frac{\Delta r}{\Delta z}\right) - \bar{v}\right]^2 \Delta z = 0$$

If the substitutions do not satisfy this equation, another guess as to the shock angle must be made, and an iteration devised such that this equation is finally satisfied.

After convergence, the final properties of point SP2 are used in conjunction with the properties of the next point up along characteristic B to compute the next point on characteristic C, and so on as before until the boundary is reached.

CHAPTER IV
SAMPLE PROBLEM

I. GENERAL CONSIDERATIONS

There has been some recent experimental work done in the area of high temperature gasdynamics using an arc heater as an energy source and argon as the gas. At AEDC work is progressing on a study to determine the feasibility of accelerating a high temperature jet with an electric field for possible wind tunnel application. Though the primary interest is in the effects of the magnetohydrodynamic forces, knowledge of the plume structure without electrical effects is of considerable importance

II. SOLUTION

Workers with arc heaters have, in general, been interested in jets exhausting from a sonic nozzle in the temperature range of 14,000 to 20,000°K at a pressure of the order of 0.01 to 1 atmospheres into an ambience at a pressure of from one-eighth to one-fiftieth of the exit pressure.

Figure 9 shows the plume resulting from the following exit conditions without radiation assuming the flow is frozen at the exit equilibrium conditions:

1. Mach number = 1.01.
2. Exit pressure = 33.42 pounds per square foot.

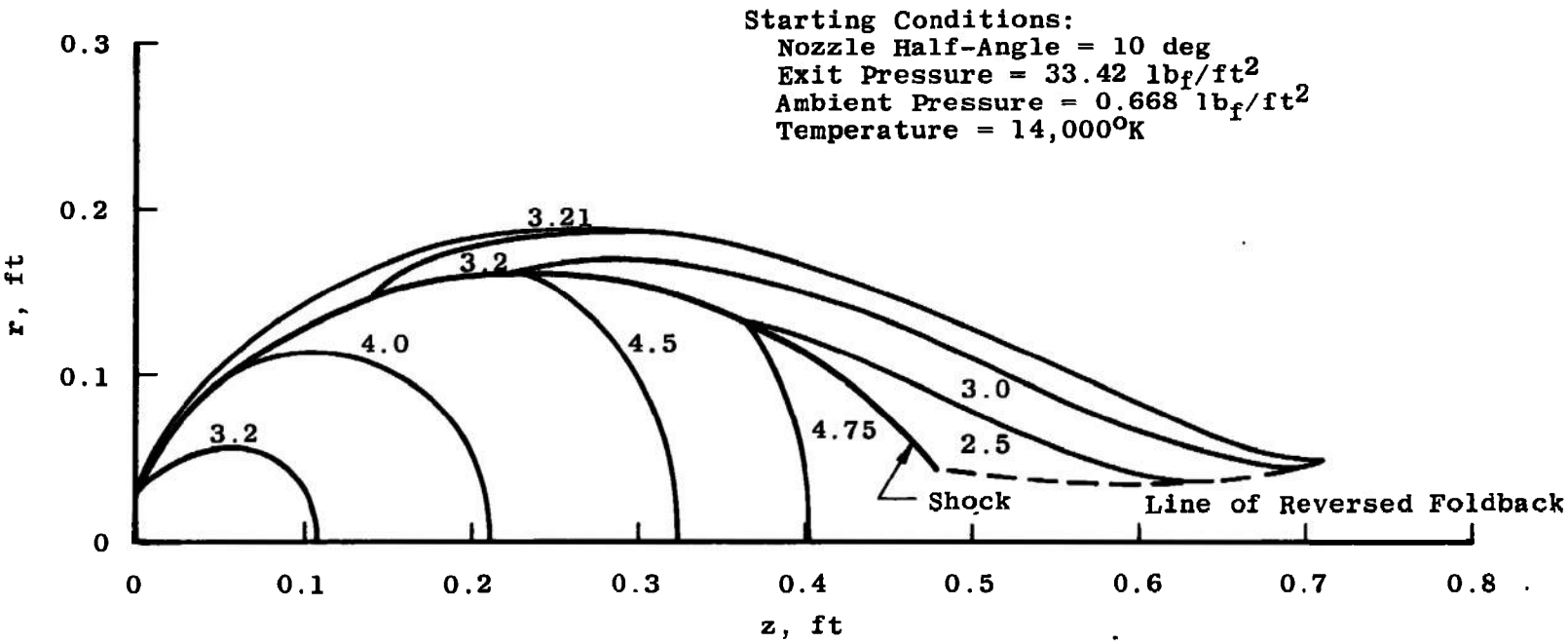

Fig. 9 Plume with Negligible Radiation Effect Showing Lines of Constant Mach number

3. Ambient pressure = 0.668 pounds per square foot.
4. Temperature = 14,000°K.
5. Nozzle radius = 0.02625 feet.

Including radiation with the above starting conditions had negligible effect. The difference was so small that it was impossible to plot.

Consider Figure 10, the Eastman and Radtke method for locating the Mach disc, as discussed in Chapter II, failed in this case since the computer program terminated before the minimum point on the pressure plot occurred. The program terminated because a crossing of left running characteristics was occurring indicating that another shock was trying to form along the dashed line in Figure 9. The program cannot handle this reversed foldback. It would be of no value to have the program construct this shock as in the actual plume the Mach disc and its attendant subsonic region would be found somewhere in this region.

In order to find a significant radiation effect, the pressures and temperature were raised. The following case then was run both with and without radiation to demonstrate the non-isoenergetic solution:

1. Mach number = 1.01.
2. Exit pressure = 2116.22 pounds per square foot.
3. Ambient pressure = 264.53 pounds per square foot.
4. Temperature = 20,000°K.
5. Nozzle radius = 0.02625 feet.

Here again the flow was assumed frozen at equilibrium exit

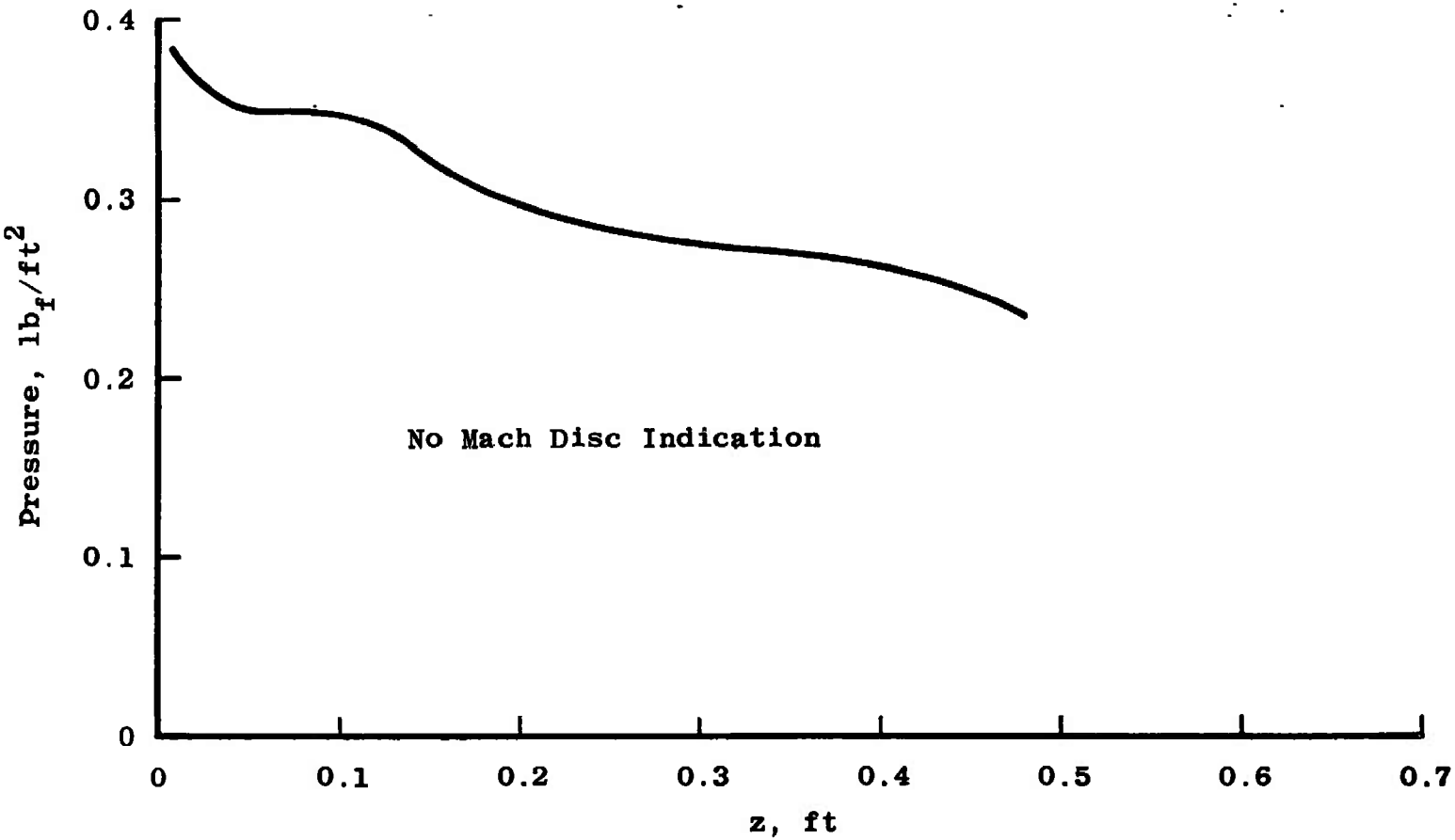

Fig. 10 Pressure Distribution Behind Embedded Shock for Case with Little Radiation Effect

conditions. Though here it is not possible to justify frozen flow on physical grounds, it becomes justifiable when the primary interest is in changes in the major features of the flow field and computer time is at a premium. Thus, though the program can handle equilibrium flow with facility, the required computer time differs from that for frozen flow by an order of magnitude.

Comparing Figure 11 with Figure 12, the radiation effects are apparent. Though the plume shape and the location of the embedded shock change little, there is a definite shift in the constant Mach number lines. The shift is most apparent in the higher density region of the upper field. The flow near the axis, however, is more easily analyzed. There, as would be expected, the energy loss due to the radiation raises the Mach number at a particular location. This is so since the radiation tends to lower the temperature thus lowering the acoustic speed while affecting the velocity very little. The upper field is more complex in that a streamline will pass from a lower number to a higher one then back to a lower Mach number. In general it can be said that when passing to the higher Mach number, the flow reaches the higher Mach number sooner with radiation. Similarly when passing to a lower Mach number, the reaching of the lower Mach number is delayed somewhat with radiation.

In Figures 13 and 14, the Eastman and Radtke criterion was used to locate the Mach disc. The method could not be applied with assurance in Figure 13 as the curve did not have a unique minimum point. The curve with radiation did, however, have a unique minimum. The apparent effect of the radiation was the shifting of the Mach disc

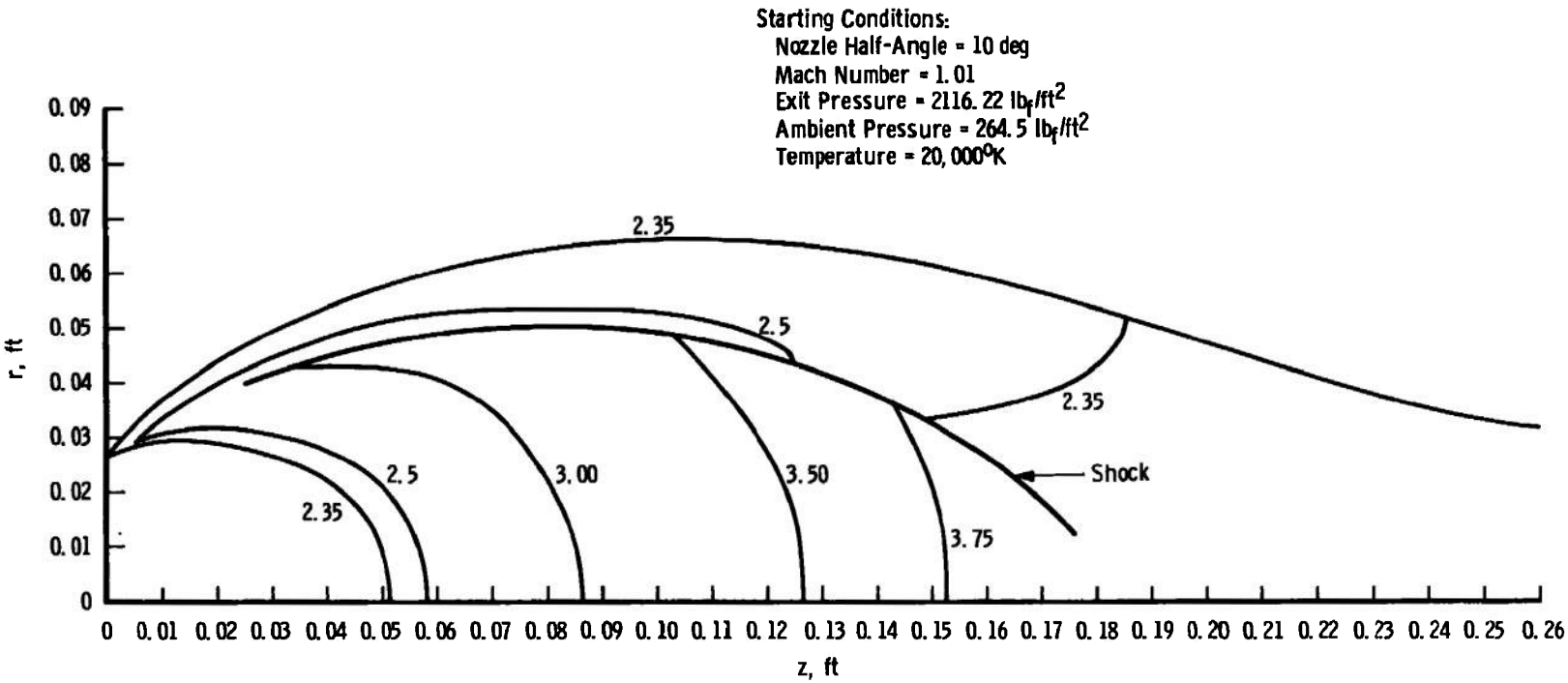

Fig. 11 Plume without Radiation Showing Lines of Constant Mach Number

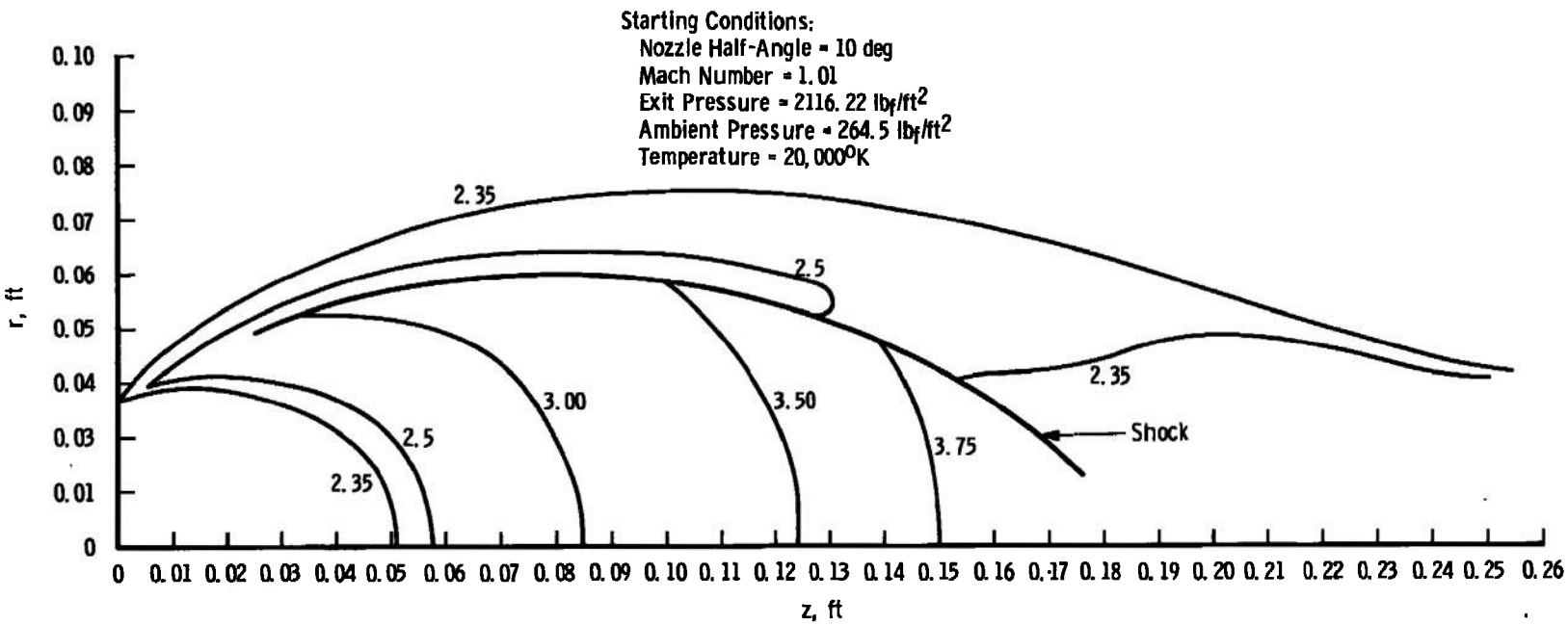

Fig. 12 Plume with Radiation Showing Lines of Constant Mach Number

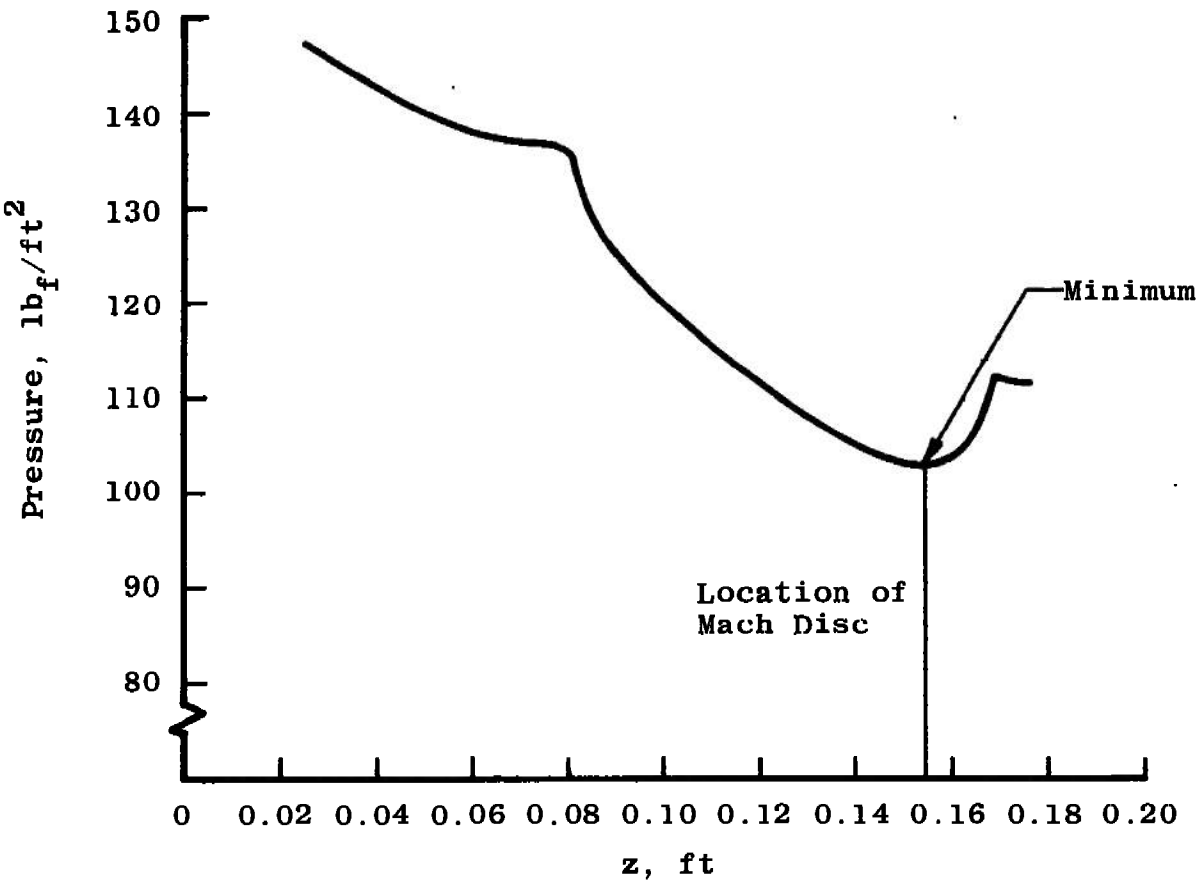

Fig. 13 Pressure Distribution Behind Embedded Shock for Case with No Radiation

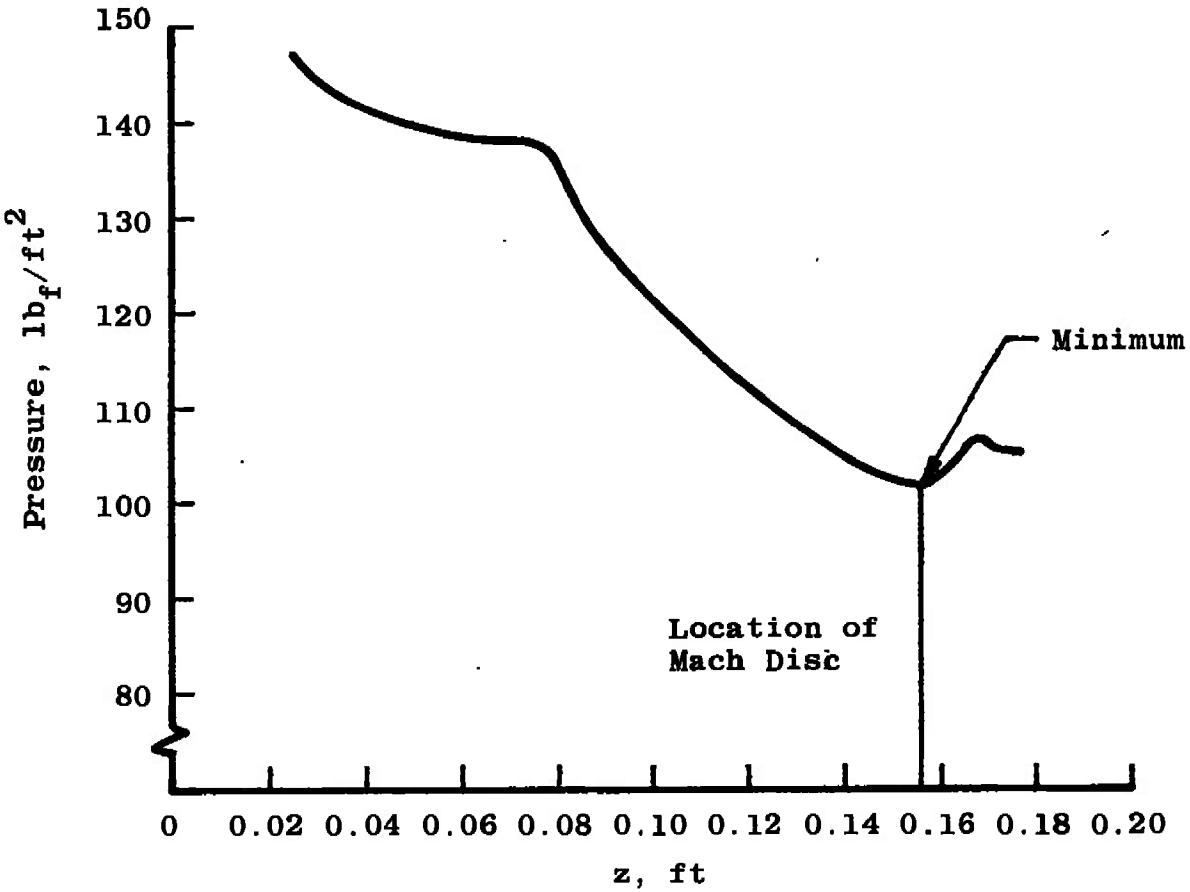

Fig. 14 Pressure Distribution Behind Embedded Shock for Case with Radiation

downstream. The reason for this effect is not obvious.

As to the accuracy of the method, it can only be said that the results with no radiation agree very well with the results in Reference (11) and other method of characteristics solutions which are too numerous to list.

Due to the confusion in the literature as to just what constitutes a good radiation model, it can only be concluded that the results agree qualitatively with what one expects to occur. That is, the direction of shift of the constant Mach number lines and the increase of radiation effect with temperature and pressure are as what would be expected.

CHAPTER V
CONCLUSIONS AND RECOMMENDATIONS

The following conclusions are made as a result of this study:

1. Even though the inclusion of the non-isoenergetic term in the energy equation and the inclusion of the embedded shock into the method of characteristics solution greatly complicates the numerical procedures involved, the resulting computer program is much more flexible and provides a more physically correct solution.
2. The use of the non-isoenergetic solution has been demonstrated by comparison of flows with and without radiation. These comparisons show that radiation has little effect on the flow except at relatively high density, i.e. in the temperature range 15,000 to 20,000°K, the radiation is not important except at pressures of the order of one-half atmosphere or above.

The following recommendations are made for future studies:

1. A study should be made to correlate the non-isoenergetic solution with experiments leading, perhaps, to a better dissipation model.
2. The computer program should be further developed so as to handle walls and center bodies, thus making the program useful in supplementing nozzle studies where real gas effects are important.

BIBLIOGRAPHY

1. Ashkenas, Harry and Frederick S. Sherman. "The Structure and Utilization of Supersonic Free Jets in Low Density Wind Tunnels." Fourth Symposium on Rarefied Gas Dynamics. Toronto: Academic Press, 1966. Pp. 84-105.

2. Loper, F. C. and M. B. Lightsey. "Characteristic Equations for a Supersonic Flow Problem with Magnetohydrodynamic Effects." Arnold Engineering Development Center Technical Report AEDC-TR-66-206, Air Force Systems Command, Arnold Air Force Station, Tennessee, January, 1966.

3. Barzelay, Martin E. "Continuum Radiation from Partially Ionized Argon," AIAA Journal, Vol. 4, No. 5, May 1966, pp. 815-822.

4. Evans, D. L. and R. S. Tankin. "Measurements of Emission and Absorption of Radiation by an Argon Plasma," The Physics of Fluids, Vol. 10, No. 6, June 1967, pp. 1137-1144.

5. Emmons, Howard W. "Arc Measurement of High-Temperature Gas Transport Properties," The Physics of Fluids, Vol. 10, No. 6, June 1967, pp. 1125-1136.

6. McGregor, W. K., Jr., M. T. Dooley, and L. E. Brewer. "Diagnostics of a Plasma Flame Exhausting to Atmospheric Pressure," Arnold Engineering Development Center Technical Report AEDC-TR-61-16, Air Force Systems Command, Arnold Air Force Station, Tennessee, January, 1962.

7. Vincenti, Walter G. and Charles H. Kruger, Jr. Introduction to Physical Gasdynamics. New York, New York: John Wiley and Sons, Inc., 1965.

8. Moore, Charlotte E. Atomic Energy Levels. Vol. I of National Bureau of Standards, United States Department of Commerce, Circular 467. 3 vols. Washington: Government Printing Office, 1949.

9. D'Attore, L. and F. Harshbarger. "The Behavior of the Mach Disc up to Moderate Pressure Ratios," General Dynamics Astronautics Report GD/A - DBE-64-042, July, 1964.

10. Eastman, D. W. and L. P. Radtke. "Location of the Normal Shock Wave in the Exhaust Plume of a Jet," AIAA Journal, Vol. 1, No. 4, April 1963, pp. 918-919.

11. Moe, Mildred M. and B. Andreas Troesch. "The Computation of Jet Flows with Shocks." Space Technology Laboratories Technical Report TR-59-0000-00661, Space Technology Laboratories, Inc., Los Angeles, California, May, 1959.

UNCLASSIFIED
Security Classification

DOCUMENT CONTROL DATA - R & D

(Security classification of title, body of abstract and indexing annotation must be entered when the overall report is classified)

1. ORIGINATING ACTIVITY *(Corporate author)*
Arnold Engineering Development Center
ARO, Inc., Operating Contractor
Arnold Air Force Station, Tennessee

2a. REPORT SECURITY CLASSIFICATION
UNCLASSIFIED

2b. GROUP
N/A

3. REPORT TITLE
AXIALLY SYMMETRIC, INVISCID, REAL GAS, NON-ISOENERGETIC FLOW SOLUTION BY THE METHOD OF CHARACTERISTICS

4. DESCRIPTIVE NOTES *(Type of report and inclusive dates)*
June 1967 through June 1968 - Final Report

5. AUTHOR(S) *(First name, middle initial, last name)*
John H. Fox, ARO, Inc.

6. REPORT DATE	7a. TOTAL NO. OF PAGES	7b. NO. OF REFS
January 1970	60	11

8a. CONTRACT OR GRANT NO.	9a. ORIGINATOR'S REPORT NUMBER(S)
F40600-69-C-0001	
b. Program Element 65401F	AEDC-TR-69-184
c.	9b. OTHER REPORT NO(S) *(Any other numbers that may be assigned this report)*
d.	N/A

10. DISTRIBUTION STATEMENT
This document has been approved for public release and sale; its distribution is unlimited.

11. SUPPLEMENTARY NOTES	12. SPONSORING MILITARY ACTIVITY
Available in DDC.	Arnold Engineering Development Center, Arnold AF Station, Tennessee 37389

13. ABSTRACT

A numerical procedure is presented for the solution of the characteristic equations for a non-isoenergetic, supersonic, real gas jet expanding into a constant pressure ambience. Included is a procedure for inserting the expansion fan and the embedded shock. Examples are given for high temperature argon jets with radiation.

DD FORM 1 NOV 65 1473

UNCLASSIFIED
Security Classification

14. KEY WORDS	LINK A		LINK B		LINK C	
	ROLE	WT	ROLE	WT	ROLE	WT
gases						
gas flow						
argon						
supersonic flow						
equations						
pressure						